HISTORICAL BIOLOGY
https://doi.org/10.1080/08912963.2022.2032024

Taylor & Francis
Taylor & Francis Group

Revisiting body size trends and nursery areas of the Neogene megatooth shark, *Otodus megalodon* (Lamniformes: Otodontidae), reveals Bergmann's rule possibly enhanced its gigantism in cooler waters

Kenshu Shimada[a,b,c], Harry M. Maisch IV[d,e], Victor J. Perez[f,g], Martin A. Becker[h] and Michael L. Griffiths[h]

[a]Department of Environmental Science and Studies, DePaul University, Chicago, Illinois, USA; [b]Department of Biological Sciences, DePaul University, Chicago, Illinois, USA; [c]Sternberg Museum of Natural History, Fort Hays State University, Hays, Kansas, USA; [d]Department of Biology and Department of Physics and Mathematics, Bergen Community College, Paramus, New Jersey, USA; [e]Department of Biological Sciences, Fairleigh Dickinson University, Madison, NJ, USA; [f]Department of Paleontology, Calvert Marine Museum, Solomons, Maryland, USA; [g]Department of Environmental Studies, St. Mary's College of Maryland, St. Mary's City, Maryland, USA; [h]Department of Environmental Science, William Paterson University of New Jersey, Wayne, New Jersey, USA

ABSTRACT

The late Neogene megatooth shark, *Otodus megalodon*, is known mainly from its gigantic teeth and possibly reached 18–20 m in total length (TL). We re-examine the previously proposed body size trends and nursery areas of *O. megalodon* by confining the previously used samples to upper anterior teeth offering more reliable TL estimates, and by taking paleolatitudes and sea-surface temperatures into consideration. We demonstrate that individuals of *O. megalodon* are on average larger in cooler water than those in warmer water – a pattern attributable to Bergmann's rule showing a latitudinal body size gradient at least for the eastern Pacific late Miocene and the western Atlantic early Pliocene assemblages. While it is still possible that neonatal *O. megalodon* could have utilised nursery areas, the previously identified paleo-nursery areas based on body size may reflect temperature-dependent trends rather than the inferred reproductive strategy. Thus, the gigantism of *O. megalodon* in cooler waters was possibly further enhanced by its cooler environment. If so, the corollary of this study is that not all populations of *O. megalodon* likely grew to gigantic sizes equally, where the common notion that the species reached 18–20 m TL should be applied primarily to populations in cooler environments.

ARTICLE HISTORY
Received 26 August 2021
Accepted 17 January 2022

KEYWORDS
Climate; fossil record; latitude; oceanography; population; shark tooth

Introduction

The megatooth shark, *Otodus megalodon* (Lamniformes: Otodontidae) is an iconic extinct shark in the late Neogene marine fossil record (e.g. Cappetta 2012; Pimiento and Balk 2015; Pimiento et al. 2016; Boessenecker et al. 2019; Perez et al. 2019, 2021). This species is known primarily from teeth and was previously placed in various genera such as the white shark genus *Carcharodon* (Lamnidae) as well as *Carcharocles, Procarcharodon*, and *Megaselachus*, but it is now often regarded as a species of *Otodus* to avoid direct phylogenetic linkage to *Carcharodon* or Lamnidae (Ehret et al. 2012) and *Otodus* non-monophyly (Shimada et al. 2017; but see also Kent 2018; Miller et al. 2021). It has been estimated to reach about 18–20 m in total length (TL) (e.g. Pimiento and Balk 2015; Nelson et al. 2016; Razak and Kocsis 2018; Pimiento et al. 2019; Cooper et al. 2020; Herraiz et al. 2020; Perez et al. 2021). The largest TL estimates for *O. megalodon* were derived from isolated teeth found in South Carolina, USA (Shimada 2019; Perez et al. 2021).

Pimiento et al. (2010) examined a population of *Otodus megalodon* from a Miocene deposit in Panama characterised by comparably small teeth, and they suggested the site to represent a nursery area for young individuals. Subsequently, Herraiz et al. (2020) examined a large dataset of the fossil record (544 teeth) of *O. megalodon* made available by Pimiento and Balk (2015, supplemental material) and identified five of the nine specific populations of *O. megalodon* examined to be nursery areas due to the abundance of smaller (i.e. younger) individuals. However, the dataset included 45 teeth yielding TL estimates >15 m, that were considerably large for their methods used (i.e. 'CH method': see below and Shimada 2019). This observation prompted us to re-examine the studies of Herraiz et al. (2020) as well as Pimiento and Balk (2015). Among their 544 examined teeth, the 45 specimens that resulted in TL estimates >15 m were all represented by tooth positions that are known to yield TL values with greater uncertainty (i.e. 'lateral teeth' that are often assigned to a wide range of tooth positions, such as L1–L5) or positions that overestimate TL (i.e. 'lower teeth'). The most reliable individual tooth-based TL estimates for *O. megalodon* are offered by upper anterior teeth (Shimada 2019; Perez et al. 2021). All 120+ specimens decisively identified as upper anterior teeth in the studies by Pimiento and Balk (2015) and Herraiz et al. (2020) resulted in TL estimates of <15 m. The purpose of this present paper is two-fold: 1) to re-examine the propositions concerning populations of *O. megalodon* put forward by Pimiento et al. (2010), Pimiento and Balk (2015), and Herraiz et al. (2020) based on a renewed look at their original data; and 2) to report and discuss a curious body size pattern across different populations of *O. megalodon* that has never been reported to date.

CONTACT Kenshu Shimada kshimada@depaul.edu Department of Environmental Science and Studies, DePaul University, 1110 West Belden Avenue, Chicago, Illinois 60614, USA; Department of Biological Sciences, DePaul University, 2325 North Clifton Avenue, Chicago, Illinois 60614, USA; Sternberg Museum of Natural History, Fort Hays State University, Hays, Kansas 67601, USA

Supplemental data for this article can be accessed here

Materials and methods

Besides 25 additional teeth collected from the 'Langhian outcrops' of northeastern Spain, Herraiz et al.'s (2020) data come directly from Pimiento and Balk's (2015) dataset. To estimate the TL of each *Otodus megalodon* individual, they used Shimada's (2003) linear regression equations showing the relationships between the tooth crown height and TL in the extant white shark (*Carcharodon carcharias*), that was the only reasonable TL estimation method available at that time. In this study, we excluded the following samples in the dataset presented by Pimiento and Balk (2015) and Herraiz et al. (2020) in order to generate a dataset that is comparable to Herraiz et al.'s (2020) study while minimising less reliable data for our analysis: 1) all teeth that were not part of the nine assemblages (= populations) of *O. megalodon* specifically examined by Herraiz et al. (2020); 2) all samples that are not identified as the upper first or second anterior teeth ('A1-A2'; i.e. excluded all lateral teeth as well as lower anterior teeth for reasons described in the Introduction); 3) samples with uncertain chronostratigraphic-stage data; and 4) samples with uncertain catalogue status (i.e. catalogue numbers bearing acronyms 'DJB', 'AT', and 'CTPA', that are not explained in Pimiento and Balk's (2015) paper). These criteria left a total of 80 decisively identified upper anterior teeth, where we refined the 'age' data presented by Pimiento and Balk (2015) based on Herraiz et al. (2020). The data used for this study are given in the Supplementary Material of this paper.

The nine assemblages of *Otodus megalodon* examined are: 1) Temblor Formation assemblage in southern California, USA (n = 11); 2) Calvert Formation assemblage in Maryland, USA (n = 8); 3) the 'Langhian outcrop' assemblage in northeastern Spain (n = 4); 4) Pisco Formation assemblage in Peru (n = 11); 5) Gatún Formation assemblage in Panama (n = 6); 6) Chucunaque Formation assemblage in Panama (n = 11); 7) Bahía Inglesa Formation assemblage in Chile (formerly the Huarra Formation; n = 16); 8) Yorktown Formation assemblage in North Carolina, USA (n = 4); and 9) Bone Valley 'Formation' assemblage in Florida, USA (technically the Bone Valley Member of the Peace River Formation; n = 9). Each assemblage consists of samples with excellent (stage-level) stratigraphic control (Table 1), although samples in the Pisco Formation (Peru) assemblage represent an aggregate of three sub-assemblages: the Serravallian sub-assemblage, Tortonian sub-assemblage, and latest Tortonian–earliest Messinian sub-assemblage. It should be noted that the Bone Valley assemblage may be locally late Miocene in age (Scott 1988, 1990), but we consider the specimens used in this study to be early Pliocene in age as originally reported by Pimiento and Balk (2015) and Herraiz et al. (2020). For the purpose of this study, the nine assemblages are classified into three 'climatic time bins': 1) the 'mid-Miocene' bin for the Langhian representing the peak period of the Middle Miocene Climatic Optimum (MMCO; i.e. hottest period relative to the other two bins); 2) 'late Miocene' bin for the Serravallian–Messinian representing the period of declining temperature (i.e. 'warm' period relative to the other two bins); and 3) 'early Pliocene' bin for the Zanclean representing a period of further decline in temperature (i.e. coolest period relative to the other two bins) (see Zachos et al. 2001; Westerhold et al. 2020; Table 1). Based on the new dataset (Supplementary Material), two analyses are conducted.

Our first analysis is to examine whether or not the pattern of differences in TL distributions across the nine assemblages of *Otodus megalodon* demonstrated by Herraiz et al. (2020) would still hold true even though the sample size for each assemblage is significantly reduced in our dataset due to the removal of samples other than upper anterior teeth. Body size trends are evaluated using Shimada's (2019) crown height (CH) based method ('CH method' herein; specifically the equation for upper anterior teeth, TL = 11.788·CH + 2.143) as well as the Perez et al. (2021) summed crown width (SCW) based method ('SCW method' herein). The SCW method results in two TL estimates for each individual tooth: one using the most complete 'large' individual (UF-VP-311000) and another using the most complete 'small' individual (CH-31-46P) (see Perez et al. 2021). However, much of our discussion below will be based on the TL estimations using the CH method, because that is nearly identical to Shimada's (2003) method used by Pimiento and Balk (2015) and Herraiz et al. (2020) for their TL estimations, where the same overall conclusions of this study can be drawn also on the basis of the SCW method.

Our second analysis is to examine whether or not there are any patterns in body size trends based on our new dataset, given that less 'noise' in the data is expected due to the use of TL estimates exclusively based on upper anterior teeth from the nine assemblages. We specifically revisit the Pimiento and Balk (2015) study that examined possible body size trends in *Otodus megalodon* across hemispheres, ocean basins, and latitudes, as well as through time, using the nine assemblages. One major aspect of our study that differs from Pimiento and Balk's (2015) study is that we translate latitudinal data into sea-surface temperature data. This is because the examined nine assemblages of *O. megalodon* chronologically span from the 'hot' MMCO to the 'cool' early Pliocene time,

Table 1. Data table showing nine assemblages of *Otodus megalodon* (see Figure 1) sorted by operational 'climatic time bin' (abbreviation 'Ser.–eMes' refers to the Serravallian–early Messinian). Statistical abbreviations: *n*, sample size; *x*TL, mean estimated total length; SD, standard deviation. Asterisk (*) indicates assumption of connection with Caribbean Sea–Atlantic Ocean (see text).

Climatic time bin Assemblage	Stage	Age	*n*	$\bar{x}$TL (SD)	Ocean/Sea	Latitude	Temperature
'Mid-Miocene' (Langhian: 'hot period')							
mM-1	Langhian	15.9–15.2 Ma	11	10.0 m (3.0)	Pacific	35°N	24°C
mM-2	Langhian	15.7–15.5 Ma	8	5.3 m (2.1)	Atlantic	39°N	23°C
mM-3	Langhian	14.2–14.0 Ma	4	4.3 m (1.4)	Mediterranean	41°N	22°C
'Late Miocene' (Serravallian–Messinian: 'warm period')							
lM-1	Ser.–eMes.	14.0–6.7 Ma	11	10.7 m (1.4)	Pacific	14–15°S	28.5°C
lM-2	Tortonian	10.9–10.7 Ma	6	5.4 m (1.9)	Pacific*	8°N	29°C
lM-3	Tortonian	10.0–9.5 Ma	11	7.4 m (2.4)	Pacific*	8°N	29°C
lM-4	Messinian	7.6–6.8 Ma	16	11.7 m (1.2)	Pacific	27°S	25°C
Early Pliocene (Zanclean: 'cool period')							
eP-1	Zanclean	5.0–4.7 Ma	9	5.9 m (2.4)	Atlantic	27°N	24°C
eP-2	Zanclean	4.8–3.1 Ma	4	10.1 m (1.4)	Atlantic	35°N	21°C

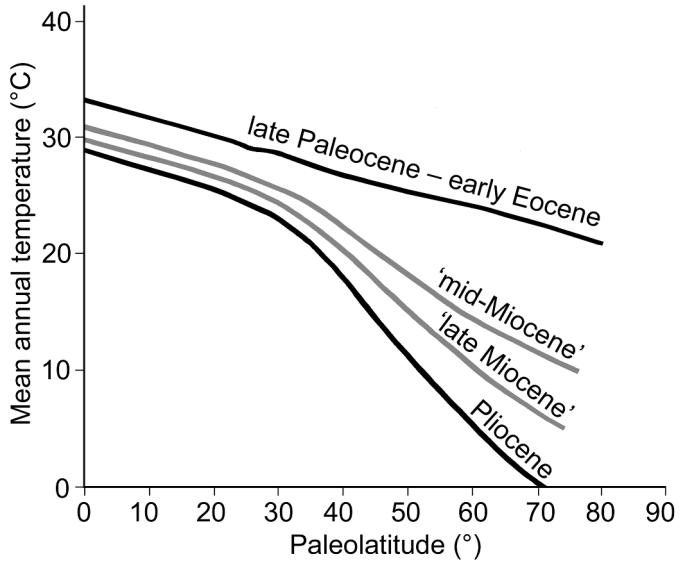

Figure 1. Relationship between paleolatitude and mean annual sea-surface temperature by different time bins (modified after Zhang et al. 2019, figure 4A; 'mid-Miocene' and 'late Miocene' refer to Langhian and Serravallian–Messinian, respectively, for the purpose of this study). Black lines = lines presented by Zhang et al. (2019); grey lines = lines developed for the purpose of this study (see text for detail).

making climatic differences due to latitudinal differences important factors to take into consideration for more meaningful comparisons. To adjust the latitude-based temperature differences through the geologic interval, we use Zhang et al.'s (2019, figure 4A) study that showed the relationship between paleolatitudes and mean annual sea-surface temperatures (Figure 1). Zhang et al. (2019) did not include data from the Miocene, but presented a line for 'late Paleocene–early Eocene' corresponding to the time frame of the Early Eocene Climatic Optimum (EECO) and a line for the 'Pliocene.' Because the sea-surface temperature during MMCO is about half-way between the EECO and Pliocene time (Zachos et al. 2001), we plotted a line half-way between the two lines to represent the relationship between paleolatitudes and mean annual sea-surface temperatures for our 'mid-Miocene' time bin. An additional line was plotted half-way between that 'mid-Miocene' line and Zhang et al.'s (2019) Pliocene line to represent a proxy line for our 'late Miocene' time bin. It should be noted that there are many other papers that provide the relationship between paleolatitudes and mean annual sea-surface temperatures (e.g. von der Heydt and Dijkstra 2006; Chan et al. 2011; Roberts et al. 2011; Contoux et al. 2012; Jones et al. 2013; Burls et al. 2021); however, the scope of those studies is generally confined to a specific age or a narrow time interval unlike Zhang et al.'s (2019) study that included both the 'late Paleocene–early Eocene' and Pliocene lines useful for our purpose. Although the exact position of each of our two extrapolated lines is hypothetical where it could have been slightly higher or lower in reality than depicted in the diagram, they are assumed to be sufficiently robust for the aim of this study. In fact, even if Zhang et al.'s (2019) lines are also only considered as proxies, they do not affect our overall analysis because it should be emphasised that the overall relative positional relationships among the four lines (Figure 1) are more important than specific paleolatitudinal or mean annual sea-surface temperature values offered by each of these lines.

Results

'Mid-Miocene' assemblages

Assemblages from the Temblor Formation of California, Calvert Formation of Maryland, and 'Langhian outcrop' of Spain represent the 'mid-Miocene' time bin, where all of them occur along or in different ocean basins (i.e. Pacific, Atlantic, and Mediterranean, respectively; Figure 2; Table 1). All three assemblages are found to be situated in the mid-latitudinal zone in the Northern Hemisphere (35°–41°N) with mean annual temperatures ranging from 22°C to 24°C after the paleolatitudinal adjustments (Figure 1; Table 1). The mean estimated total lengths of *Otodus megalodon*, using the CH method, from the Temblor Formation, Calvert Formation, and the Spanish 'Langhian outcrop' are 10.0, 5.3, and 4.3 m, respectively (Figure 2; Table 1). The mean TL estimates, based on the SCW method with the 'large' individual as the analogue, for the same localities are 16.1, 9.3, and 5.3 m, respectively. Mean TL estimates, based on the SCW method with the 'small' individual as the analogue, for the same localities are 14.8, 8.5, and 5.1 m, respectively.

'Late Miocene' assemblages

Assemblages from the Pisco Formation in Peru, Gatún Formation in Panama, Chucunaque Formation in Panama, and Bahía Inglesa Formation in Chile belong to the 'late Miocene' time bin in this study, all of which are distributed longitudinally along the western margin of Central and South America (note: although the Gatún Formation assemblage may technically represent a Caribbean assemblage (Pimiento et al. 2013), it is referred to as one of the 'Pacific' assemblages in our discussion below for simplicity, including the fact that the connection existed between the Atlantic–Caribbean and Pacific (Coates and Stallard 2013; Bacon et al. 2015; Jaramillo 2018) and that it does not affect the main conclusions of this study; Figure 2; Table 1). After the paleolatitudinal adjustments (Figure 1), the Gatún Formation and Chucunaque Formation assemblages are found to be both located at 8°N (i.e. close to 9.1°N estimated by Anderson et al. 2017) with an estimated mean annual temperature of 29°C, whereas the latitude and estimated mean annual temperature for the Pisco Formation and Bahía Inglesa Formation are found to be 14–15°S with 28.5°C and 27°S with 25°C, respectively (Figure 1; Table 1). The mean estimated total lengths of *O. megalodon*, based on the CH method, from the Pisco, Gatún, Chucunaque, and Bahía Inglesa formations are 10.7, 5.4, 7.4, and 11.7 m, respectively (Figure 2(a); Table 1). The mean TL estimates, based on the SCW method with the 'large' individual as the analogue, for the same localities are 15.3, 7.6, 10.2, and 17.8 m, respectively. Mean TL estimates, based on the SCW method with the 'small' individual as the analogue, for the same localities are 14.1, 7.0, 9.4, and 16.6 m, respectively.

Early Pliocene assemblages

Assemblages from the Yorktown Formation in North Carolina and Bone Valley 'Formation' in Florida represent the 'early Pliocene' time bin. Both occur along the western Atlantic in the Northern Hemisphere (Figure 2; Table 1), where the Yorktown and Bone Valley assemblages are found to be situated at 35°N and 27°N with mean annual temperatures of 21°C and 24°C, respectively, after the paleolatitudinal adjustments (Figure 1; Table 1). The mean estimated total lengths of *Otodus megalodon*, using the CH method, from the Yorktown

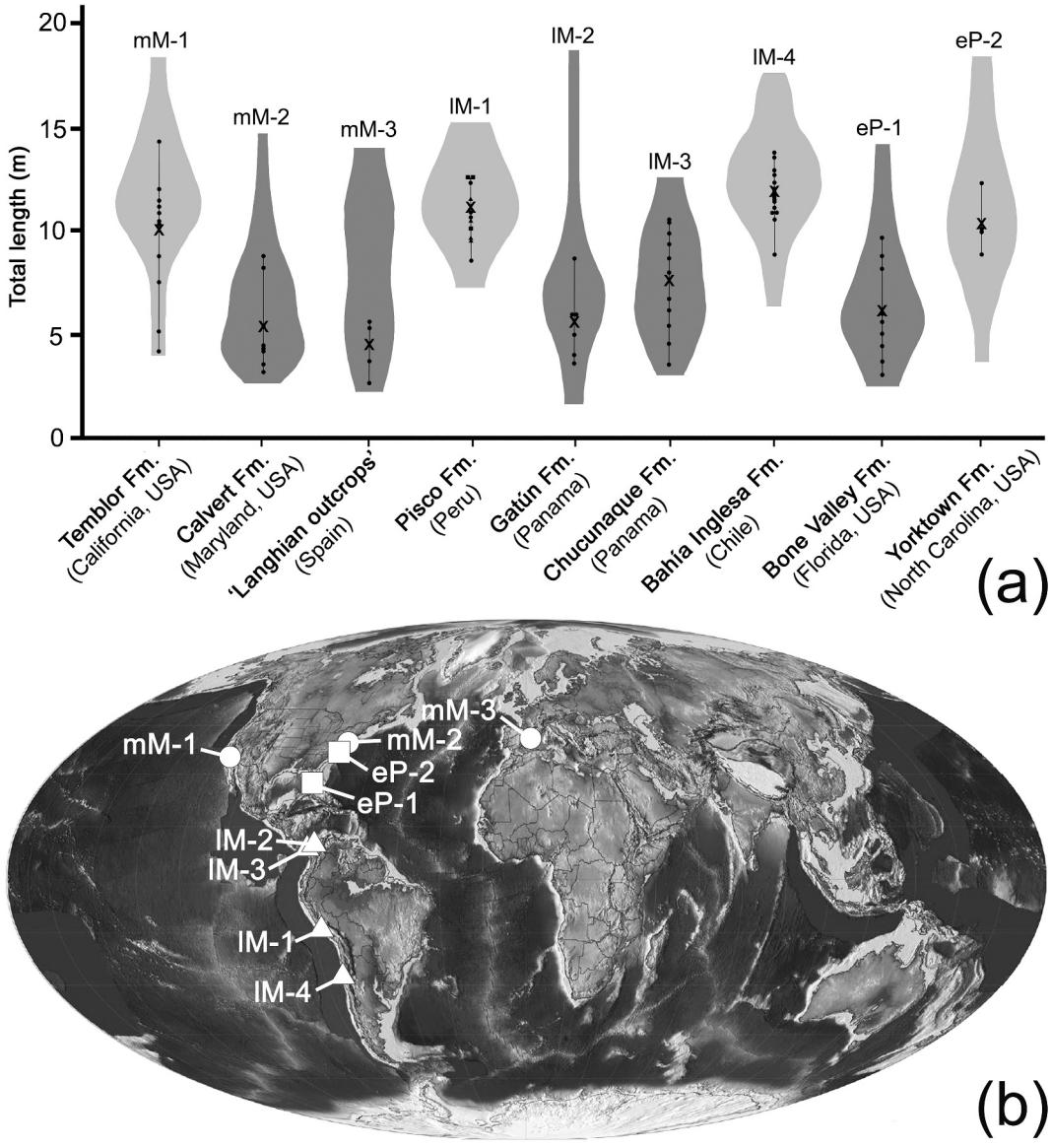

Figure 2. Nine assemblages of *Otodus megalodon* re-examined in this study (see text and Table 1 for detail). (a) Distribution of estimated total lengths (TL) of *Otodus megalodon* based on crown heights of teeth at each assemblage; violin plots represent Herraiz et al.'s (2020, figure 2) data, where 'darker violins' represent assemblages identified as nursery areas by Herraiz et al. (2020); black plots connected with a line represent data in this present study (see Supplementary Material for data), where each plot represents each tooth sample and each X-mark indicates average TL for that respective assemblage (for IM-1, circles represent samples from the Serravallian, triangles from the Tortonian, and squares from the latest Tortonian–earliest Messinian). (b) 'Late Neogene' palaeogeographic map showing location of each assemblage (circles represent 'mid-Miocene ['mM': Langhian] assemblages, triangles 'late Miocene' ['IM': Serravallian–Messinian] assemblages, and squares early Pliocene ['eP': Zanclean] assemblages; palaeogeographic map based on Map 5 [Serravallian–Tortonian] of Scotese 2014).

Formation is 10.1 m, whereas from the Bone Valley 'Formation' is 5.9 m (Figure 2; Table 1). The mean TL estimates, based on the SCW method with the 'large' individual as the analogue, for the Yorktown and Bone Valley 'formations' are 15.5 m and 8.5 m, respectively. Mean TL estimates, based on the SCW method with the 'small' individual as the analogue, for the same formations are 14.3 m and 7.8 m, respectively.

Discussion

Like most other extinct sharks, *Otodus megalodon* is largely known only from its well-mineralised teeth in the fossil record (e.g. Cappetta 2012; Shimada et al. 2020). Thus, examination of its tooth proportions has been the primary means to infer its body size (e.g. Randall 1973; Gottfried et al. 1996; Razak and Kocsis 2018; Shimada 2019; Perez et al. 2021). Pimiento and Balk (2015) used a large sample (n = 544 teeth) to examine possible body size trends in *O. megalodon* across hemispheres, ocean basins, and latitudes, as well as through time. They noted: 'Collectively, these specimens suggest that [*O.*] *megalodon* body size differs significantly between hemispheres and among ocean basins, but not across a latitudinal gradient' (p. 485) and 'that the differences in [*O.*] *megalodon* body size across space are maintained throughout time' (p. 486). Pimiento and Balk's (2015) data included those from the Miocene Gatún Formation of Panama, which was previously recognised as a paleo-nursery area of *O. megalodon* based on the small tooth sizes of the species representing the assemblage (Pimiento et al. 2010).

Subsequently, Herraiz et al. (2020) reported four additional probable paleo-nursery areas of *O. megalodon*. They were the Calvert Formation assemblage in Maryland, 'Langhian outcrop' assemblage in Spain, Chucunaque Formation assemblage in Panama, and Bone Valley 'Formation' assemblage in Florida, which quantitatively had smaller mean tooth sizes than the other four assemblages they examined: the Temblor Formation assemblage in California, Pisco Formation assemblage in Peru, Bahía Inglesa Formation assemblage in Chile, and Yorktown Formation assemblage in North Carolina.

Even though our present study is based on a significantly reduced sample size for each assemblage (see Materials and Methods), remarkably, the overall total length distribution pattern across the nine assemblages between Herraiz et al.'s (2020) study and ours is found to be nearly identical, where the mean estimated total length of *Otodus megalodon* for the Calvert Formation, 'Langhian outcrop', Gatún Formation, Chucunaque Formation, and Bone Valley 'Formation' assemblages are found to be consistently smaller than Temblor Formation, Pisco Formation, Bahía Inglesa Formation, and Yorktown Formation assemblages (Figure 2(a)). Although the SCW method yields larger TL estimates than the CH method, the same trend is also observed even if body length estimates based on the SCW method are used (see Supplementary Material). However, one factor that was not considered by Pimiento and Balk (2015) and Herraiz et al. (2020) was the time-corrected, latitude-based mean annual sea-surface temperature for each examined *O. megalodon* assemblage.

Although our extrapolated paleolatitude-to-temperature lines for the 'mid-Miocene' and late Miocene are tentative (Figure 1), we recognise some noteworthy patterns, where we collectively refer all four 'late Miocene' assemblages as 'Pacific assemblages' for simplicity even through the Gatún Formation assemblage may technically represent a Caribbean assemblage (see above). For example, the mean estimated TL increases from the low latitude assemblages (Gatún and Chucunaque formations: 8°N – i.e. near the equator) to the high latitude assemblages (Bahía Inglesa Formation being the southernmost assemblage: 27°S) with decreasing mean sea-surface temperatures from 29°C to 25°C ($y = -1.222x - 40.070$, where x represents mean sea-surface temperature and y represents mean TL, with $r^2 = 0.551$ and $p = 0.258$, where $n = 4$; note the negative slope of the linear equation) (Figure 3). It is worth noting that, although the four assemblages span more than seven million years, the average of the three sub-assemblages constituting the Pisco Formation assemblage are similar; thus, influences associated with the diachronous nature of the four assemblages within the 'late Miocene' time bin are likely to be negligible. Likewise, the two 'early Pliocene' assemblages that occur along the western Atlantic Ocean, the Yorktown and Bone Valley assemblages, also show the same pattern where the lower-latitude (27°N) Bone Valley assemblage with a warmer mean annual sea-surface temperature (24°C) consists of teeth from overall smaller individuals (5.9 m TL on average) than the Yorktown assemblage at a higher latitude (35°N) with a cooler environment (21°C) ($y = -1.400x + 39.500$, where x represents mean sea-surface temperature and y represents mean TL, with $r^2 = 1$ and $p = 0$ because of $n = 2$; note the negative slope of the linear equation) (Figure 3). Furthermore, the Calvert Formation assemblage ('mid-Miocene') and Yorktown Formation assemblage (early Pliocene) are geographically close on the global scale, yet the Yorktown Formation representing a cool-period assemblage with a mean sea-surface annual temperature of 21°C produces larger teeth on average than teeth from the Calvert Formation representing a hot-period assemblage with a mean sea-surface annual temperature of 23°C. In short, individuals of *O. megalodon* are on average larger in cooler water than those in warmer or hotter water, where this pattern is consistent with the concept referred to as Bergmann's rule – i.e.

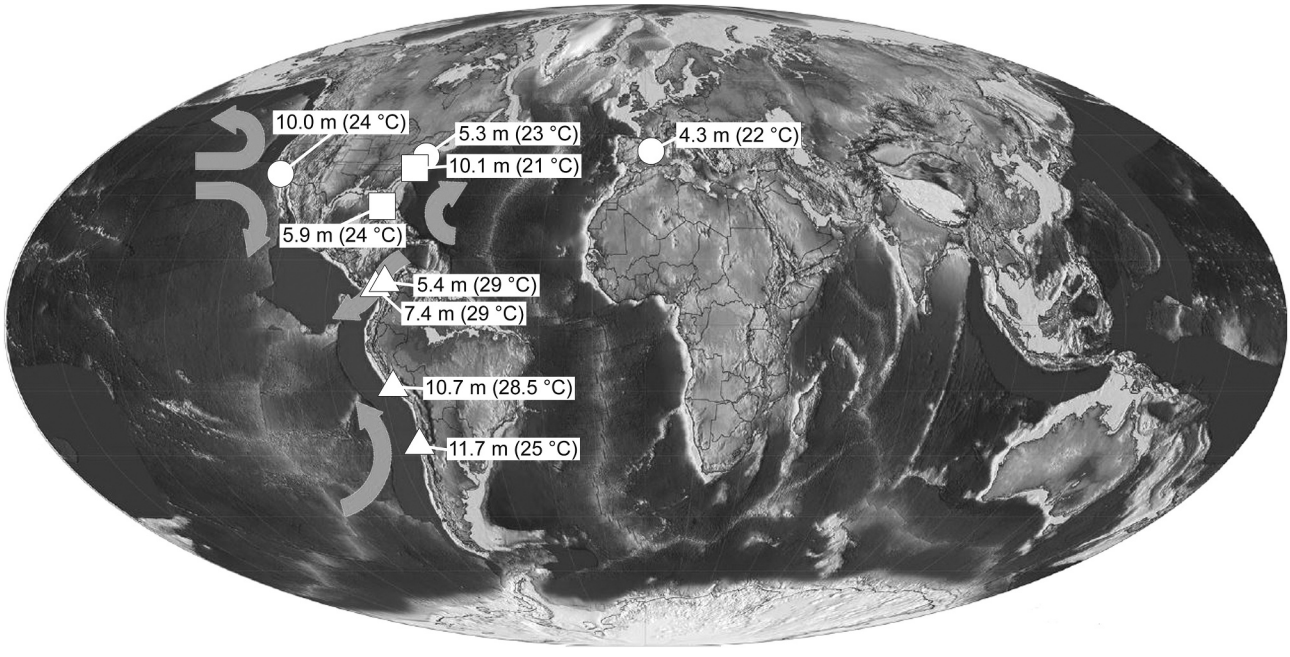

Figure 3. 'Late Neogene' palaeogeographic map showing the distribution of the eight examined assemblages with mean estimated total length of *Otodus megalodon* and sea-surface temperature at each site (see Figure 1(b); Table 1) and arrows indicating select prevailing oceanic currents relevant to this study (palaeogeographic map based on Map 5 [Serravallian–Tortonian] of Scotese (2014); arrow mark on the Atlantic Ocean is of early Pliocene current based on Karas et al. (2017, figure 4a); all other arrows are of middle Miocene currents based on Herold et al. (2012, figure 2b).

latitudinal gradient of increasing body size in animals with increasing latitude (Bergmann 1847; for review, see Meiri and Dayan (2003); Huston and Wolverton (2011)).

Bergmann's rule is regarded as a valid generalisation, which was originally proposed to explain a broad trend that larger animals are advantageous in cooler climates because of their ability to retain heat more efficiently due to their small surface-to-volume ratio compared to smaller animals (e.g. see Huston and Wolverton (2011) and Meiri (2011) and references therein). Although the most representative examples of Bergmann's rule come from extant and extinct terrestrial mammals (e.g. Ashton et al. 2000; Huston and Wolverton 2011; Lomolino et al. 2012; Secord et al. 2012; Smith 2012; Saarinen et al. 2014), the rule has also been recognised in a wide range of non-mammalian vertebrates including fishes, amphibians, reptiles, and birds (see Millien et al. (2006) and references therein). However, it should be noted that Bergmann's rule is technically not about latitude, but rather about some ecological attributes correlated with latitudinal gradients, where multiple factors besides temperature could have been the ultimate causes that are correlative between body size and latitude (Huston and Wolverton 2011). One major proposed cause is the role of net primary production (NPP) of terrestrial plants (McNab 2010) that may also have cascading effects to the ecological productivity in marine environments through soil or nutrient runoff, although other factors, such as population density and species richness, affect body sizes of marine organisms as well (Huston and Wolverton 2011). Nevertheless, large megatooth sharks (e.g. *Otodus megalodon* and *O. chubutensis*) are known to have fed on marine mammals, such as cetaceans and pinnipeds (e.g. Aguilera et al. 2008; Collareta et al. 2017; Godfrey et al. 2018, 2021), where at least in the present-day oceans, latitudinal body size gradients following Bergmann's rule are well documented in these marine mammals (Torres-Romero et al. 2016) and among many other marine vertebrates including fishes (e.g. Millien et al. 2006; Fernández-Torres et al. 2018; Saunders and Tarling 2018; Izzo and Gillanders 2020). To our knowledge, Bergmann's rule has not been explicitly reported for any living elasmobranchs, but latitudinal body size gradient data consistent with the rule do exist for the starspotted smooth-hound shark, *Mustelus manazo* (Yamaguchi et al. 1998). It should be noted that the current lack of any decisive example of comparable modern elasmobranch analogues should not be taken as evidence for our contention to be false, especially given the fact that there is no comparable extant shark to *O. megalodon* (e.g. see Shimada et al. 2020, 2021). Whereas water temperature is known to at least affect the onset of sexual maturity in the cloudy catshark (*Scyliorhinus torazame*: Horie and Tanaka 2002) and the growth rate in the Port Jackson shark (*Heterodontus portusjacksoni*: Izzo and Gillanders 2020) that have a significant bearing to changing climate through time, our study may well represent the first possible case of Bergmann's rule demonstrated for elasmobranchs if our data interpretation is correct.

The gigantism of *Otodus megalodon* is thought to have been attained through the evolution of its regional endothermy, a thermophysiological trait to be able to maintain certain areas of the body at higher temperatures than the ambient water (Ferrón 2017), where the evolution of regional endothermy in certain fishes, including some modern lamniform sharks such as lamnids (*Lamna, Isurus*, and *Carcharodon*), is closely linked to their fast cruising speed (Harding et al. 2021). Therefore, it is possible that the observed latitude-based body size pattern of *O. megalodon* in each time bin may be correlated with a poleward body size increase. Some contemporaneous clades of marine mammals (e.g. *Eubalaena*) may have also achieved gigantism through a combination of factors related to Bergmann's rule (Bisconti et al. 2021), so perhaps *O. megalodon* enhanced its predatory success through endothermically powered fast swimming along with poleward gigantism. Regardless of the exact cause(s) or mechanism(s) for the body size pattern conforming to Bergmann's rule (e.g. Meiri 2011), the latitude-based body size pattern elucidated in this study is new for *O. megalodon*. In fact, it constitutes a newly recognised potential ecological driver for the gigantism in *O. megalodon*, if not an evolutionary one.

In this study, the mid-Miocene Calvert Formation assemblage is compared to the early Pliocene Yorktown Formation assemblage above, but it should be noted that the three 'mid-Miocene' assemblages representing assemblages at a similar mid-latitudinal zone (35–41°N) collectively do not show the pattern suggesting Bergmann's rule ($y = 2.850x - 59.017$, where x represents mean sea-surface temperature and y represents mean TL, with $r^2 = 0.877$ and $p = 0.228$, where $n = 3$; e.g. note the positive slope of the linear equation) (Figure 3). However, it is important to emphasise that direct comparisons among the three 'mid-Miocene' assemblages are difficult because they come from three completely different ocean basins with different oceanic conditions. For instance, where the Temblor Formation assemblage of California exhibits the widest TL range among the nine examined assemblages (Figure 2(a)), it is the only location among the nine assemblages where the prevailing oceanic current perpendicularly strikes the coastline, rather than sweeps parallel to the coastline (Figure 3). The exact reason is uncertain, but it is possible that this location could have had higher NPP relative to the other two examined mid-Miocene sites as a result of coastal upwelling (e.g. White et al. 1992; Xiu et al. 2018), along with soil or nutrient runoff from land to sea, that could have resulted in large body sizes of animals including *Otodus megalodon* (see above; Huston and Wolverton 2011). Teeth of *O. megalodon* from the 'Langhian outcrop' assemblage of Spain come from the overall smallest individuals (4.3 m TL on average) compared to any other examined assemblages, despite the extrapolated sea-surface temperature being relatively cool (22°C: Table 1) (note: Rosen (1999) examined Mediterranean coral associations and determined the minimum sea-surface temperatures during the Langhian–Serravallian to be 18–20°C, which is not significantly different from our interpretation of 22°C for the Langhian outcrop assemblage). The extremely small average TL may be due to a rather small sample size of teeth (n = 4), but it could also be due to a quite different paleoenvironment in the Mediterranean compared to the Atlantic and Pacific oceans. While the connection between the Mediterranean and Atlantic Ocean was established during the Langhian (Krijgsman et al. 1999; Herold et al. 2012; Gibert et al. 2013; Hamon et al. 2013), it is in the realm of possibility to hypothesise that the Mediterranean, along with the Paratethys, could have represented a relatively enclosed environment, possibly leading to insular dwarfism of *O. megalodon*. Regardless, the Langhian outcrop (with anomalously small mean TL) and Temblor Formation (with the widest TL range) assemblages have unique TL distributions, possibly suggesting the presence of overall TL differences across different local populations of *O. megalodon*, besides the latitude-based sea-surface temperature differences. It should be added that it is for this reason that the nine geographically (and chronologically) mixed assemblages examined in this study (Table 1; Figure 3) should not be collectively compared together, and that it likely explains why there is practically no relationship between the mean sea-surface temperature and mean TL if the nine assemblages are analysed altogether (i.e. $y = 0.065x + 6.229$, where x represents mean sea-surface temperature and y represents mean TL, with $r^2 = 0.005$ and $p = 0.854$, where $n = 9$; note the considerably small r^2-value and large p-value). Although no significant differences in sea-surface temperatures between the

Northern and Southern hemispheres exist (Belkin 2009; Fisher et al. 2010), direct comparisons among the nine assemblages would be particularly problematic because there is a large difference in the amount of land between the Northern and Southern hemispheres that is also thought to contribute to asymmetry in fish size, among other biological factors such as NPP and species richness (Huston and Wolverton 2011).

The fact that the 'small-bodied assemblages' as well as 'large-bodied assemblages' are found in all three time bins suggests that the body size distribution of *Otodus megalodon* was largely maintained throughout time. The temperature-dependent TL distribution pattern we recognise, at least for the four 'Pacific assemblages' during the 'late Miocene' and the two 'Atlantic assemblages' during the 'early Pliocene', suggests that the body size of *O. megalodon* is smaller in areas with warmer sea-surface temperatures than cooler areas, and that Bergmann's rule holds true for two significantly diachronous assemblages (i.e. the mid-Miocene Calvert Formation and the early Pliocene Yorktown Formation). This implies that not only did *O. megalodon* simply maintain its body size throughout time, but it also maintained the temperature-dependent body size pattern throughout time.

Our study may seem to refute the existence of paleo-nursery areas of *Otodus megalodon* put forward by Pimiento et al. (2010) and Herraiz et al. (2020). Yet, the temperature-dependent body size pattern does not necessarily preclude the possibility of the existence of nursery areas based on the fossil record. For example, it is still plausible that assemblages near the equator like those of the Gatún and Chucunaque formations could have been nursery areas where individuals began to migrate out to higher latitude regions represented by the Pisco Formation and Bahía Inglesa Formation assemblages as they grew larger. However, this 'migration hypothesis' is difficult to support for the Calvert Formation assemblage dominated by smaller individuals given that it represents an assemblage located at the highest latitude (41°N; Table 1) among the nine assemblages. This fact in turn also reduces the support for the nursery area hypothesis for *O. megalodon*, unless one or more undocumented assemblages dominated by larger individuals existed northward with the assumption that nursery areas could have been widespread during the MMCO including the Calvert Formation assemblage. While nursery areas benefit taxa with small neonates (Castro 1993; Beck et al. 2001; Heupel et al. 2018), whether or not such nursery areas were necessary for neonatal *Otodus megalodon*, already about 2 m at birth likely due to its reproductive strategy as a lamniform shark (oophagous embryos: Shimada et al. 2020, 2021) needs further investigation.

Our present study is based on a significantly reduced sample size for each assemblage compared to Herraiz et al.'s (2020) study, and one may question whether such a small sample size for each locality would accurately characterise its TL distribution. In particular, it is likely that the differences in depositional environment among different localities would have led to different taphonomic effects and processes that would have affected the fossilisation potential of teeth at each locality. Furthermore, it is also possible that different museum collections used for sampling is likely manifested with different levels of collecting bias, where smaller sample sizes may be especially prone to inaccurate characterisation of each assemblage. However, it should be emphasised that the nature of the overall TL distribution pattern across the nine assemblages in Herraiz et al.'s (2020) work is almost identical to ours; that is, the mean estimated total lengths of *Otodus megalodon* at the five localities considered to represent as nursery areas by Herraiz et al. (2020) are found to be smaller than the other four localities (Figure 2(a)). The exclusive use of upper anterior teeth in our study constrained body length estimates to a smaller range; however, the range of estimates maintained the same pattern across localities as was found by Herraiz et al. (2020). Likewise, the smallest teeth from the five paleo-nursery areas are all consistently smaller than the smallest teeth from the other four localities. Furthermore, the same body size distribution pattern is present even if the SCW method is used (Supplementary Materials). All these factors indicate that the same conclusions drawn from our study can be derived from Herraiz et al.'s (2020) data if the same set of time-corrected, latitude-based mean annual sea-surface temperatures used in this study (Figure 1; Table 1) is applied to their data.

The findings of this study are significant because they show that body size in animals is known to affect a wide range of their fitness-related traits. Such traits include the range of travelling distances, tolerance level to extreme environmental conditions, forage (e.g. predatory) successes, mortality (e.g. predation) risks, oxygen demands, and energy storage capacity, besides the extent of heat retention (e.g. Peters 1986; Kram and Taylor 1990; Cohen et al. 1993; Hone and Benton 2005; Speakman 2005; Brown and Sibly 2006; Huston and Wolverton 2011; Healy et al. 2013; Ahti et al. 2020). Nevertheless, the observations and propositions made in this paper should be tested with a larger sample size for each assemblage as well as including more assemblages of *O. megalodon* worldwide in the future, particularly from the Eastern Hemisphere. Besides further evaluation of potential taphonomic differences and collecting biases for each assemblage (see above), some other possible issues across different assemblages to consider include potential biotic (e.g. predators and competitors) and abiotic (e.g. salinity and dissolved oxygen) ecological pressures as well as the latitude- and temperature-based differences in the size and types of potential food sources for *O. megalodon*. Nevertheless, revisiting the previously proposed body size trends and nursery areas (Pimiento et al. 2010; Pimiento and Balk 2015; Herraiz et al. 2020) has revealed the possibility that *O. megalodon* exhibited the body size trends consistent with Bergmann's rule through time and space during its existence in the Neogene. If indeed the rule applied to *O. megalodon*, the notion that the fossil species reached at least 15 m TL (Shimada 2019), and possibly as much as 18–20 m TL (Perez et al. 2021), would be expected to primarily occur in populations that inhabited cooler waters that were typically at higher latitudes. This proposition holds true as the largest previously estimated individuals of *O. megalodon* are from relatively high latitudes (i.e. North Carolina, South Carolina, and Chile: Shimada 2019; Perez et al. 2021).

Conclusions

In this present study, we re-examined the body size trends and possible nursery areas proposed by Pimiento and Balk (2015) and Herraiz et al. (2020) by removing specimens with tenuous data. Although our study is based on significantly reduced sample sizes, the overall TL distribution pattern across the nine assemblages examined by Herraiz et al. (2020) was found to be nearly identical to that of our study. However, neither Pimiento and Balk's (2015) nor Herraiz et al.'s (2020) studies took mean annual sea-surface temperatures across different paleolatitudes into consideration. By taking the time-corrected and latitude-based mean annual sea-surface temperatures into consideration, we found that individuals of *Otodus megalodon* were on average larger in cooler waters relative to those in warmer waters – a pattern attributable to Bergmann's rule. Almost all previously identified possible paleo-nurseries of *O. megalodon* characterised by smaller individuals inferred from smaller teeth were found to be at warmer regions or time frames. One exception was the 'Langhian outcrop' assemblage in Spain that represented the sole example of a Mediterranean

population in our dataset, that is inferred to have had a unique environment compared to the other examined assemblages all located along either the Atlantic or Pacific Oceans.

Pimiento and Balk (2015) found the differences in the body size of *Otodus megalodon* across space are maintained throughout time but found no significant latitudinal gradient. The fact that both the 'small-bodied assemblages' and 'large-bodied assemblages' are found in all three time bins we examined (i.e. mid-Miocene, late Miocene, and early Pliocene) suggest that the overall body size distribution in *O. megalodon* was indeed largely maintained throughout time. However, we found an observable latitudinal gradient of body size at least for the late Miocene assemblages along the eastern Pacific Ocean and the early Pliocene assemblages along the western Atlantic Ocean. Therefore, our data suggest that not only did *O. megalodon* simply maintain its body size throughout time, but it also maintained the temperature-dependent body size pattern throughout time. In addition, although it is still possible that neonatal *O. megalodon* could have utilised nursery areas, our study suggests that the previously identified paleo-nursery areas of the fossil species may not necessarily represent actual paleo-nursery areas.

Previously, regional endothermy was proposed to be the evolutionary driver for the gigantism of *Otodus megalodon* (Ferrón et al. 2017). Harding et al. (2021) revealed that endothermy in fishes evolved to increase their swimming speed, rather than to expand their thermal niche. If Bergmann's rule indeed applies to the body size trend in *O. megalodon*, we contend that the gigantism of *O. megalodon* in cooler waters was further enhanced by its cooler environment – a newly identified possible ecological driver for the gigantism in *O. megalodon*. In addition, our study suggests that the notion that *O. megalodon* reached at least 15 m TL (Shimada 2019), and possibly as much as 18–20 m TL (Perez et al. 2021), should be applied primarily to individuals that lived in cooler waters.

Acknowledgments

This research was funded in part by a National Science Foundation Sedimentary Geology and Paleobiology Award to KS (Award Number 1830858), and MLG and MAB (Award Number 1830581). We thank E. Kast and A. Akhtar (Princeton University) for their discussion with us on extinct and extant sharks. In addition, various support provided by the Department of Environmental Science and Studies and Department of Biological Sciences at DePaul University is appreciated. We also thank the three anonymous reviewers for their constructive comments and suggestions that significantly improved the quality of this paper. As a postscript, the idea about possible latitude-dependent differences in body size of *Otodus megalodon* in this present study stems from H. Shimada who caught a 50-cm-TL mangrove snapper (*Lutjanus griseus*: Actinopteygii, Perciformes) in the Florida Keys. The 'big catch' led to the discussion about its age estimate and 'where do large fish live?' where T. Shimada called KS and MABs' attention on a paper that different populations of mangrove snapper have different growth parameters, leading to the discussion about the potential size differences among different populations of *O. megalodon*.

Disclosure statement

No potential conflict of interest was reported by the author(s).

Funding

This work was supported by the National Science Foundation Sedimentary Geology and Paleobiology Award [1830581,1830858].

References

Aguilera OA, García L, and Cozzuol MA. 2008. Giant-toothed white sharks and cetacean trophic interaction from the Pliocene Caribbean Paraguaná Formation. Paläont Z. 82(2):204–208. doi:10.1007/BF02988410.

Ahti PA, Kuparinen A, Uusi-Heikkilä S. 2020. Size does matter—the eco-evolutionary effects of changing body size in fish. Environ Rev. 28 (3):311–324. doi:10.1139/er-2019-0076.

Anderson BM, Hendy A, Johnsone EH, Allmon WD. 2017. Paleoecology and paleoenvironmental implications of turritelline gastropod-dominated assemblages from the Gatun Formation (Upper Miocene) of Panama. Palaeogeogr Palaeoclimatol, Palaeoecol. 470:132–146. doi:10.1016/j.palaeo.2017.01.026.

Ashton KG, Tracy MC, and de Queiroz A. 2000. Is Bergmann's rule valid for mammals? Am Nat. 156(4):390–415. doi:10.1086/303400.

Bacon CD, Silvestro D, Jaramillo CA, Smith BT, Chakrabarty P, Antonelli A. 2015. Biological evidence supports an early and complex emergence of the Isthmus of Panama. Proc Nat Acad Sci. 112(19):6110–6115. doi:10.1073/pnas.1423853112.

Beck MW, Heck KL, Able KW, Childers DL, Eggleston DB, Gillanders BM, Halpern B, Hays CG, Hoshino K, and Minello TJ, et al. 2001. The identification, conservation, and management of estuarine and marine nurseries for fish and invertebrates: a better understanding of the habitats that serve as nurseries for marine species and the factors that create site-specific variability in nursery quality will improve conservation and management of these areas. BioScience. 51:633–641. doi:10.1641/0006-3568(2001)051[0633:TICAMO]2.0.CO;2.

Belkin IM. 2009. Rapid warming of large marine ecosystems. Prog Oceanogr. 81 (1–4):207–213. doi:10.1016/j.pocean.2009.04.011.

Bergmann C. 1847. Ueber die verha¨ltnisse der wa¨rmeo¨konomie der thiere zu ihrer gro¨sse. Gottinger Studien. 3:595–708.

Bisconti M, Pellegrino L, and Carnevale G. 2021. Evolution of gigantism in right and bowhead whales (Cetacea: Mysticeti: Balaenidae). Biol J Linn Soc. 134 (2):498–524. doi:10.1093/biolinnean/blab086.

Boessenecker RW, Ehret DJ, Long DJ, Churchill M, Martin E, Boessenecker SJ. 2019. The early pliocene extinction of the mega-toothed shark *Otodus megalodon*: a view from the eastern North Pacific. PeerJ. 7:e6088. doi:10.7717/peerj.6088.

Brown JH, Sibly RM. 2006. Life-history evolution under a production constraint. Proc Natl Acad Sci. 103(47):17595–17599. doi:10.1073/pnas.0608522103.

Burls NJ, Bradshaw CD, De Boer AM, Herold N, Huber M, Pound M, Donnadieu Y, Farnsworth A, Frigola A, Gasson E, et al. 2021. Simulating Miocene warmth: insights from an opportunistic multi-model ensemble (MioMIP1). Paleoceanogr Paleoclimatol. 36(5):e2020PA004054. doi:10.1029/2020PA004054.

Cappetta H. 2012. Chondrichthyes. Mesozoic and Cenozoic Elasmobranchii: teeth. In: Schultze H-P, editor. Handbook of paleoichthyology (Vol. 3E). Munich: Verlag Dr. Friedrich Pfeil; p. 1–512.

Castro JI. 1993. The shark nursery of Bulls Bay, South Carolina, with a review of the shark nurseries of the southeastern coast of the United States. Environ Biol Fish. 38(1–3):37–48. doi:10.1007/BF00842902.

Chan WL, Abe-Ouchi A, Ohgaito R. 2011. Simulating the mid-Pliocene climate with the MIROC general circulation model: experimental design and initial results. Geoscientific Model Develop. 4(4):1035–1049. doi:10.5194/gmd-4-1035-2011.

Coates AG, Stallard RF. 2013. How old is the Isthmus of Panama? Bull Mar Sci. 89(4):801–813. doi:10.5343/bms.2012.1076.

Cohen JE, Pimm SL, Yodzis P, Saldaña J. 1993. Body sizes of animal predators and animal prey in food webs. J Anim Ecol. 1(1):67–78. doi:10.2307/5483.

Collareta A, Lambert O, Landini W, Di Celma C, Malinverno E, Varas-Malca R, Urbina M, and Bianucci G. 2017. Did the giant extinct shark *Carcharocles megalodon* target small prey? Bite marks on marine mammal remains from the late Miocene of Peru. Palaeogeog, Palaeoclimat, Palaeoecol. 469:84–91. doi:10.1016/j.palaeo.2017.01.001.

Contoux C, Ramstein G, and Jost A. 2012. Modelling the mid-Pliocene warm period climate with the IPSL coupled model and its atmospheric component LMDZ5A. Geoscientific Model Develop. 5(3):903–917. doi:10.5194/gmd-5-903-2012.

Cooper JA, Pimiento C, Ferrón HG, Benton MJ. 2020. Body dimensions of the extinct giant shark *Otodus megalodon*: a 2D reconstruction. Sci Rep. 10 (1):14596. doi:10.1038/s41598-020-71387-y.

Ehret DJ, MacFadden BJ, Jones DS, Devries TJ, Foster DA, and Salas-Gismondi R. 2012. Origin of the white shark *Carcharodon* (Lamniformes: Lamnidae) based on recalibration of the Upper Neogene Pisco Formation of Peru. Palaeontology. 55(6):1139–1153. doi:10.1111/j.1475-4983.2012.01201.x.

Fernández-Torres F, Martínez PA, Olalla-Tárraga MÁ. 2018. Shallow water ray-finned marine fishes follow Bergmann's rule. Basic and Applied Ecology. 33:99–110. doi:10.1016/j.baae.2018.09.002.

Ferrón H. 2017. Regional endothermy as a trigger for gigantism in some extinct macropredatory sharks. PLoS ONE. 12(9):e0185185. doi:10.1371/journal.pone.0185185.

Ferrón HG, Martínez-Perez C, Botella H. 2017. The evolution of gigantism in active marine predators. Hist Biol. 30(5):712–716. doi:10.1080/08912963.2017.1319829.

Fisher JAD, Frank KT, Leggett WC. 2010. Global variation in marine fish body size and its role in biodiversity-ecosystem functioning. Mar Ecol Prog Ser. 405:1–13. doi:10.3354/meps08601.

Gibert L, Scott GR, Montoya P, Ruiz-Sánchez FJ, Morales J, Luque L, Abella J, Lería M. 2013. Evidence for an African-Iberian mammal dispersal during the pre-evaporitic Messinian. Geology. 41(6):691–694. doi:10.1130/G34164.1.

Godfrey SJ, Ellwood M, Groff S, Verdin MS. 2018. *Carcharocles*-bitten odontocete caudal vertebrae from the coastal eastern United States. Acta Palaeont Polo. 63:463–468.

Godfrey SJ, Nance JR, Riker NL. 2021. *Otodus*-bitten sperm whale tooth from the Neogene of the Coastal Eastern United States. Acta Palaeont Polo. 66:599–603.

Gottfried MD, Compagno LJV, Bowman SC. 1996. Size and skeletal anatomy of the giant "megatooth" shark *Carcharodon megalodon*. In: Klimley AP, Ainley DG, editors. Great white sharks: the biology of *Carcharodon carcharias*. San Diego: Academic Press; p. 55–66.

Hamon N, Sepulchre P, Lefebvre V, Ramstein G. 2013. The role of eastern Tethys seaway closure in the middle Miocene climatic transition (ca. 14 Ma). Climate of the Past. 9(6):2687–2702. doi:10.5194/cp-9-2687-2013.

Harding L, Jackson A, Barnett A, Donohue I, Halsey L, Huveneers C, Meyer C, Papastamatiou Y, Semmens JM, Spencer E, et al. 2021. Endothermy makes fishes faster but does not expand their thermal niche. Function Ecol. 00:1–9. doi:10.1111/1365-2435.13869

Healy K, McNally L, Ruxton GD, Cooper N, Jackson AL. 2013. Metabolic rate and body size are linked with perception of temporal information. Anim Behav. 86(4):685–696. doi:10.1016/j.anbehav.2013.06.018.

Herold N, Huber M, Müller RD, and Seton M. 2012. Modeling the Miocene climatic optimum: ocean circulation.Paleoceanography 27:PA1209. doi:10.1029/2010PA002041.

Herraiz JL, Ribé J, Botella H, Martínez-Pérez C, and Ferrón HG. 2020. Use of nursery areas by the extinct megatooth shark *Otodus megalodon* (Chondrichthyes: Lamniformes). Biol Lett. 16(11):20200746. doi:10.1098/rsbl.2020.0746.

Heupel MR, Kanno S, Martins AP, Simpfendorfer CA. 2018. Advances in understanding the roles and benefits of nursery areas for elasmobranch populations. Mar Fresh Res. 70(7):897–907. doi:10.1071/MF18081.

Hone DW, Benton MJ. 2005. The evolution of large size: how does cope's rule work? Trends Ecol Evol. 20(1):4–6. doi:10.1016/j.tree.2004.10.012.

Horie T, Tanaka S. 2002. Geographic variation of maturity size of the cloudy catshark, *Scyliorhinus torazame*, in Japan. J Fac Mar Sci Tech-Tokai Univ, Japan. 53:111–124.

Huston MA, Wolverton S. 2011. Regulation of animal size by eNPP, Bergmann's rule, and related phenomena. Ecol Monog. 81(3):349–405. doi:10.1890/10-1523.1.

Izzo C, Gillanders BM. 2020. Port Jackson shark growth is sensitive to temperature change. Front Mar Sci. 7:240. doi:10.3389/fmars.2020.00240.

Jaramillo C. 2018. Evolution of the Isthmus of Panama: biological, paleoceanographic and paleoclimatological implications. In: Hoorn C, Antonelli A, editors. Mountains, climate and biodiversity. Oxford: John Wiley and Sons; p. 323–338.

Jones TD, Lunt DJ, Schmidt DN, Ridgwell A, Sluijs A, Valdes PJ, and Maslin M. 2013. Climate model and proxy data constraints on ocean warming across the Paleocene–Eocene Thermal Maximum. Earth-Sci. Rev. 125:123–145. doi:10.1016/j.earscirev.2013.07.004.

Karas C, Nürnberg D, Bahr A, Groeneveld J, Herrle JO, Tiedemann R, deMenocal PB. 2017. Pliocene oceanic seaways and global climate. Sci Rep. 7(1):39842. doi:10.1038/srep39842.

Kent BW. 2018. The cartilaginous fishes (chimaeras, sharks, and rays) of Calvert Cliffs. In: Godfrey SJ, editor. The geology and vertebrate paleontology of Calvert Cliffs, Maryland, USA. Washington D.C.: Smithsonian Scholarly Press; p. 45–157.

Kram R, Taylor C. 1990. Energetics of running: a new perspective. Nature. 346 (6281):265–267. doi:10.1038/346265a0.

Krijgsman W, Hilgen FJ, Raffi I, Sierro FJ, and Wilson DS. 1999. Chronology, causes and progression of the Messinian salinity crisis. Nature. 400 (6745):652–655. doi:10.1038/23231.

Lomolino MV, Sax DF, Palombo MR, van der Geer AA. 2012. Of mice and mammoths: evaluations of causal explanations for body size evolution in insular mammals. J Biogeogr. 39(5):842–854. doi:10.1111/j.1365-2699.2011.02656.x.

McNab BK. 2010. Geographic and temporal correlations of mammalian size reconsidered: a resource rule. Oecologia. 164(1):13–23. doi:10.1007/s00442-010-1621-5.

Meiri S. 2011. Bergmann's Rule—what's in a name? Glob Ecol Biogeogr. 20 (1):203–207. doi:10.1111/j.1466-8238.2010.00577.x.

Meiri S, Dayan T. 2003. On the validity of Bergmann's rule. J Biogeogr. 30:331–351.

Miller AE, Gibson ML, and Boessenecker RW. 2021. A megatoothed shark (*Carcharocles angustidens*) nursery in the Oligocene Charleston Embayment, South Carolina, USA. Palaeont Electronica. 24(2):a19. doi:10.26879/1148.

Millien V, Lyons KS, Olson L, Smith FA, Wilson AB, Yom-Tov Y. 2006. Ecotypic variation in the context of global climate change: revisiting the rules. Ecol Lett. 9(7):853–869. doi:10.1111/j.1461-0248.2006.00928.x.

Nelson JS, Grande TC, Wilson MVH. 2016. Fishes of the World. Hoboken (New Jersey): Wiley and Sons; p. 752.

Perez VJ, Godfrey SJ, Kent B, Weems R, Nance J. 2019. The transition between *Carcharocles chubutensis* and *Carcharocles megalodon* (Otodontidae, Chondrichthyes): lateral cusplet loss through time. J Vert Paleont. e1546732. doi:10.1080/02724634.2018.1546732.

Perez VJ, Leder RM, and Badaut T. 2021. Body length estimation of Neogene macrophagous lamniform sharks (*Carcharodon* and *Otodus*) derived from associated fossil dentitions. Palaeont Electronica. 24(1):a09. doi:10.26879/1140.

Peters RH. 1986. The ecological implications of body size. Cambridge (UK): Cambridge Univ Press; p. 329.

Pimiento C, Balk MA. 2015. Body-size trends of the extinct giant shark *Carcharocles megalodon*: a deep-time perspective on marine apex predators. Paleobiol. 41(3):479–490. doi:10.1017/pab.2015.16.

Pimiento C, Cantalapiedra JL, Shimada K, Field DJ, Smaers JB. 2019. Evolutionary pathways towards shark gigantism. Evolution. 73(3):588–599. doi:10.1111/evo.13680.

Pimiento C, Ehret DJ, MacFadden BJ, Hubbell G, Stepanova A. 2010. Ancient nursery area for the extinct giant shark Megalodon from the Miocene of Panama. PLoS ONE. 5(5):e10552. doi:10.1371/journal.pone.0010552.

Pimiento C, González-Barba G, Ehret DJ, Hendy AJ, MacFadden BJ, Jaramillo C. 2013. Sharks and rays (Chondrichthyes, Elasmobranchii) from the late Miocene Gatun Formation of Panama. J Paleontol. 87(5):755–774. doi:10.1666/12-117.

Pimiento C, MacFadden BJ, Clements CF, Varela S, Jaramillo C, Velez-Juarbe J, Silliman BR. 2016. Geographical distribution patterns of *Carcharocles megalodon* over time reveal clues about extinction mechanisms. J Biogeog. 43 (8):1645–1655. doi:10.1111/jbi.12754.

Randall JE. 1973. Size of the great white shark (*Carcharodon*). Science. 181 (4095):169–170. doi:10.1126/science.181.4095.169.

Razak H, Kocsis L. 2018. Late Miocene *Otodus* (*Megaselachus*) *megalodon* from Brunei Darussalam: body length estimation and habitat reconstruction. Neues Jahrb Geol Palaontol Abh. 288(3):299–306. doi:10.1127/njgpa/2018/0743.

Roberts CD, LeGrande AN, Tripati AK. 2011. Sensitivity of seawater oxygen isotopes to climatic and tectonic boundary conditions in an early Paleogene simulation with GISS ModelE-R. Paleoceanogr. 26(4). doi:10.1029/2010PA002025.

Rosen BR. 1999. Palaeoclimatic implications of the energy hypothesis from Neogene corals of the Mediterranean region. In: Agusti J, Rook L, Andrews PJ, editors. Hominoid evolution and climatic change in Europe. Cambridge (UK): Cambridge University Press; p. 309–327.

Saarinen JJ, Boyer AG, Brown JH, Costa DP, Ernest SM, Evans AR, Fortelius M, Gittleman JL, Hamilton MJ, Harding LE, et al. 2014. Patterns of maximum body size evolution in Cenozoic land mammals: eco-evolutionary processes and abiotic forcing. Proc Roy Soc B: Biol Sci. 281(1784):2013–2049.

Saunders RA, Tarling GA. 2018. Southern Ocean mesopelagic fish comply with Bergmann's rule. Am Nat. 191(3):343–351. doi:10.1086/695767.

Scotese CR. 2014. Atlas of Neogene paleogeographic maps (Mollweide projection), Maps 1–7, Vol. 1. In: The Cenoaoic, PALEOMAP Atlas for ArcGIS. Evanston, Illinois: PALEOMAP Project.

Scott T. 1988. The lithostratigraphy of the Hawthorn Group (Miocene) of Florida. Florida Geol Surv Bull. 59:1–148.

Scott T. 1990. The lithostratigraphy of the Hawthorn Group of Peninsular Florida. In: Burnett W, Riggs S, editors. Phosphate deposits of the world, Vol. 3, Neogene to modern phosphorites. Cambridge (UK): Cambridge University Press; p. 325–336.

Secord R, Bloch JI, Chester SGB, Boyer DM, Wood AR, Wing SL, Kraus MJ, McInerney FA, Krigbaum J. 2012. Evolution of the earliest horses driven by climate change in the Paleocene-Eocene Thermal Maximum. Science. 335 (6071):959–962. doi:10.1126/science.1213859.

Shimada K. 2003. The relationship between the tooth size and total body length in the white shark, *Carcharodon carcharias* (Lamniformes: Lamnidae). J Fossil Res. 35: 28–33. (date of imprint 2002).

Shimada K. 2019. The size of the megatooth shark, *Otodus megalodon* (Lamniformes: Otodontidae), revisited. Hist Biol. 33(7):904–911. doi:10.1080/08912963.2019.1666840.

Shimada K, Becker MA, and Griffiths ML. 2020. Body, jaw, and dentition lengths of macrophagous lamniform sharks, and body size evolution in Lamniformes with special reference to 'off-the-scale' gigantism of the megatooth shark, *Otodus megalodon*. Hist Biol. 33(11):2543–2559. doi:10.1080/08912963.2020.1812598.

Shimada K, Bonnan MF, Becker MA, and Griffiths ML. 2021. Ontogenetic growth pattern of the extinct megatooth shark *Otodus megalodon*—implications for its reproductive biology, development, and life expectancy. Hist Biol. 33(12):3254–3259. doi:10.1080/08912963.2020.1861608.

Shimada K, Chandler RE, Lam OLT, Tanaka T, and Ward DJ. 2017. A new elusive otodontid shark (Lamniformes: Otodontidae) from the lower Miocene, and comments on the taxonomy of otodontid genera, including the 'megatoothed' clade. Hist Biol. 29(5):704–714. doi:10.1080/08912963.2016.1236795.

Smith FA. 2012. Some like it hot. Science. 335(6071):924–925. doi:10.1126/science.1219233.

Speakman JR. 2005. Body size, energy metabolism and lifespan. J Exp Biol. 208(9):1717–1730. doi:10.1242/jeb.01556.

Torres-Romero EJ, Morales-Castilla I, Olalla-Tárraga MÁ. 2016. Bergmann's rule in the oceans? Temperature strongly correlates with global interspecific patterns of body size in marine mammals. Global Ecol. Biogeogr. 25(10):1206–1215. doi:10.1111/geb.12476.

von der Heydt A, Dijkstra HA. 2006. Effect of ocean gateways on the global ocean circulation in the late Oligocene and early Miocene. Paleoceanogr. 21(1):A1011. doi:10.1029/2005PA001149.

Westerhold T, Marwan N, Drury AJ, Liebrand D, Agnini C, Anagnostou E, Barnet JSK, Bohaty SM, De Vleeschouwer D, Florindo F, et al. 2020. An astronomically dated record of Earth's climate and its predictability over the last 66 million years. Science. 369(6509):1383–1387. doi:10.1126/science.aba6853.

White LD, Garrison RE, Barron JA. 1992. Miocene intensification of upwelling along the California margin as recorded in siliceous facies of the Monterey Formation and offshore DSDP sites. In: Summerhayes CP, Prell WL, Emeis K-C, editors. Upwelling systems; evolution since the early Miocene (Vol. 64). London (UK): Geological Society of London; p. 429–442.

Xiu P, Chai F, EN C, Castruccio FS. 2018. Future changes in coastal upwelling ecosystems with global warming: the case of the California Current System. Sci Rep. 8(1):2866. doi:10.1038/s41598-018-21247-7.

Yamaguchi A, Taniuchi T, and Shimizu M. 1998. Geographic variation in growth of the starspotted dogfish *Mustelus manazo* from five localities in Japan and Taiwan. Fish Sci. 64(5):732–739. doi:10.2331/fishsci.64.732.

Zachos J, Pagani M, Sloan L, Thomas E, Billups K. 2001. Trends, rhythms, and aberrations in global climate 65 Ma to present. Science. 292(5517):686–693. doi:10.1126/science.1059412.

Zhang L, Hay WW, Wang C, Gu X. 2019. The evolution of latitudinal temperature gradients from the latest Cretaceous through the Present. Earth-Sci Rev. 189:147–158. doi:10.1016/j.earscirev.2019.01.025.